Geometric barrier and current string in type-II superconductors obtained from continuum electrodynamics

Ernst Helmut Brandt
Max-Planck-Institut für Metallforschung, D-70506 Stuttgart, Germany
(Received 28 September 1998)

It is shown how the current density $\mathbf{J}(\mathbf{r},t)$ and magnetic induction $\mathbf{B}(\mathbf{r},t)$ in a superconductor with arbitrary shape and material laws $\mathbf{H}(\mathbf{B},\mathbf{r})$ (equilibrium field) and $\mathbf{E}(\mathbf{J},\mathbf{B},\mathbf{r})$ (electric field caused by flux-line motion) can be calculated within continuum approximation when a magnetic field $\mathbf{B_a}(\mathbf{r},t)$ and/or current are applied. This general method is then used to calculate the geometric edge barrier for flux penetration, and Indenbom's current string occurring at the flux front, for superconducting strips with rectangular cross section in a perpendicular field. The field of first flux entry $B_{\rm en}$ is given. Both effects could not be obtained by previous theories which assume $\mathbf{H}=\mathbf{B}/\mu_0$. [S0163-1829(99)00706-7]

The irreversibility of penetration and exit of magnetic flux in type-II superconductors is partly due to a geometric barrier which depends on the specimen shape and causes a hysteresis even in the absence of flux-line pinning. This edge barrier is particularly pronounced when superconductor platelets or films of constant thickness are exposed to a perpendicular magnetic field. Similarly as the microscopic Bean-Livingston barrier for the penetration of parallel flux lines into a superconducting half space,[1] the geometric barrier delays the penetration but not the exit of flux lines, leading thus to a characteristic asymmetry of the magnetization loops, which is also present in type-I superconductors.[2] Such asymmetric magnetization loops and the profiles of the magnetic induction $\mathbf{B}(\mathbf{r})$ and current density $\mathbf{J}(\mathbf{r})$ have been calculated analytically and numerically for thin superconductor strips in Refs. 3–5 by assuming an edge barrier of given height. The barrier height was recently calculated for thin strips and disks;[6,7] Ref. 7 presents a recipe for obtaining the quasistatic $\mathbf{B}(\mathbf{r}),\mathbf{J}(\mathbf{r})$, and magnetization curves for superconductors of arbitrary shape. In superconductors with rectangular cross section the edge barrier is caused by the delayed penetration of flux lines at the four corners.[3,7,8] Another interesting phenomenon predicted for superconductor strips and disks of finite thickness is Indenbom's ''current string,''[9] which occurs at the penetrating flux fronts where H is continuous but B jumps abruptly to zero.

Both the edge barrier and the current string depend on the reversible field $\mathbf{H}(\mathbf{B})=\partial F/\partial\mathbf{B}$ which causes an equilibrium induction $\mathbf{B}$ in a type-II superconductor with free-energy density $F(\mathbf{B})$. To obtain the barrier and current string, it is essential that $\mathbf{H}(\mathbf{B})$ is *not* approximated by its high-field value $\mathbf{H}\approx\mathbf{B}/\mu_0$ but saturates to $|\mathbf{H}(\mathbf{B})|\to H_{c1}$ for $\mathbf{B}\to 0$. The lower critical field H_{c1} is related to the self-energy of an isolated flux line $U_s=\Phi_0 H_{c1}$ where $\Phi_0=h/2e$ is the quantum of flux.

Recent calculations of the penetration and exit of flux in superconductor bars[10] and cylinders[11] of finite thickness with volume pinning assume $\mathbf{B}=\mu_0\mathbf{H}$ and thus cannot describe the edge barrier and current string, applying mainly to cases where $B=|\mathbf{B}|\gg B_{c1}=\mu_0 H_{c1}$ is large inside the superconductor. In the continuum description of Refs. 10 and 11, the dynamics and statics of the flux lines (i.e., pinning, thermally activated depinning, creep, and flow) enter via a general law $\mathbf{E}(\mathbf{J},\mathbf{B})$ where $\mathbf{E}$ is the local electric field generated by moving flux lines driven by the current density $\mathbf{J}$.

In this paper I present the electrodynamics of superconductors with arbitrary shape and arbitrary material laws $\mathbf{E}(\mathbf{J},\mathbf{B},\mathbf{r})$ and $\mathbf{H}(\mathbf{B},\mathbf{r})$ which may be inhomogeneous and anisotropic (by Hall effect or by material anisotropy). The superconductor is exposed to a time dependent magnetic field $\mathbf{B_a}(\mathbf{r},t)=\nabla\times\mathbf{A_a}(\mathbf{r},t)$ and/or electric field $\mathbf{E_a}(\mathbf{r},t)=-\nabla\Phi_a(\mathbf{r},t)$ that may be chosen to drive a prescribed total current via a feedback algorithm. I consider the *continuum approximation* in which the flux-line spacing $a\approx(\Phi_0/B)^{1/2}$ and the magnetic penetration depth λ are smaller than all relevant lengths. This continuum electrodynamics is then shown to yield both the edge barrier and the current string by calculating the penetration and exit of perpendicular flux in superconducting strips of rectangular cross section with finite H_{c1} and with various degrees of volume pinning.

To explain this general method I first generalize the simpler algorithm of Ref. 10, where $\mathbf{B}=\mu_0\mathbf{H}$ was assumed, to arbitrary three-dimensional (3D) geometry, allowing also for an applied current. Both methods are based on the fact that the current density $\mathbf{J}(\mathbf{r})=-\nabla^2 A_J(\mathbf{r})$ inside and at the surface of a conductor is uniquely determined by the vector potential $\mathbf{A}(\mathbf{r})=\mathbf{A_J}(\mathbf{r})+\mathbf{A_a}(\mathbf{r})$, or by the local induction $\mathbf{B}(\mathbf{r})=\nabla\times\mathbf{A}(\mathbf{r})$, *inside* the specimen volume V. With the gauge $\nabla\cdot\mathbf{A}=0$ one has

$$\mathbf{A}(\mathbf{r})=-\int_V d^3r'\,Q(\mathbf{r},\mathbf{r}')\mathbf{J}(\mathbf{r}')+\mathbf{A_a}(\mathbf{r}), \tag{1}$$

$$\mathbf{J}(\mathbf{r})=-\int_V d^3r'\,K(\mathbf{r},\mathbf{r}')[\mathbf{A}(\mathbf{r}')-\mathbf{A_a}(\mathbf{r}')]. \tag{2}$$

Here the kernel $Q(\mathbf{r},\mathbf{r}')=-\mu_0/(4\pi|\mathbf{r}-\mathbf{r}'|)$ and its inverse $K(\mathbf{r},\mathbf{r}')=Q^{-1}(\mathbf{r},\mathbf{r}')$ are *scalar*; K may be obtained by discretizing $\mathbf{r}$ on a grid with positions $\mathbf{r}_i$ and weights w_i and inverting the matrix $Q_{ij}=Q(\mathbf{r}_i,\mathbf{r}_j)w_j$.[10] The second term in Eq. (2) is the surface screening current $\mathbf{J_s}(\mathbf{r})$ that generates a field $-\mathbf{B_a}(\mathbf{r})$ inside the volume V and flows only on a sur-

face layer whose thickness is determined by the grid distance (or by the magnetic penetration depth λ if finite λ is chosen). This surface current ''tells'' the specimen about the ''outside world,'' i.e., the applied field, since all positions $\mathbf{r}$ and $\mathbf{r}'$ and integrals in this paper are restricted to the specimen volume V and use the same grid. If required for figures, the induction $\mathbf{B}(\mathbf{r})=\nabla\times\mathbf{A}(\mathbf{r})$ may be calculated from Eq. (1) at any position $\mathbf{r}$ also outside V.

In the previous method[10,11] the condition $\mathbf{B}=\mu_0\mathbf{H}$ allowed us to use the usual current density $\mathbf{J}=\mu_0^{-1}\nabla\times\mathbf{B}=-\mu_0^{-1}\nabla^2\mathbf{A}$ in the material law $\mathbf{E}=\mathbf{E}(\mathbf{J},\mathbf{B},\mathbf{r})$. Inserting this electric field into the induction law $\dot{\mathbf{B}}=-\nabla\times\mathbf{E}$ written in the form $\dot{\mathbf{A}}=-\mathbf{E_t}-\mathbf{E_a}$ [$\mathbf{E_t}$ is the ''transverse'' part of $\mathbf{E}(\mathbf{J},\mathbf{B},\mathbf{r})=\mathbf{E_t}+\mathbf{E_l}$ satisfying $\nabla\cdot\mathbf{E_t}=0$ while $\nabla\times\mathbf{E_l}=0$; $\mathbf{E_a}$ drives the applied current] and taking the time derivative of Eq. (2), one arrives at an equation of motion for $\mathbf{J}(\mathbf{r},t)$,

$$\dot{\mathbf{J}}(\mathbf{r},t)=\int_V d^3r'K(\mathbf{r},\mathbf{r}')[\mathbf{E}(\mathbf{J},\mathbf{B},r')_\mathbf{t}+\mathbf{E_a}(\mathbf{r}',t)+\dot{\mathbf{A}}_\mathbf{a}(\mathbf{r}',t)]. \tag{3}$$

Equation (3) generalizes Eq. (7) of Ref. 10 to arbitrary geometry and material law $\mathbf{E}(\mathbf{J},\mathbf{B},\mathbf{r})$. It is easily time integrated, e.g., by starting with $\mathbf{J}(\mathbf{r},0)=0$ and putting $\mathbf{J}(\mathbf{r},t+dt)=\mathbf{J}(\mathbf{r},t)+\dot{\mathbf{J}}(\mathbf{r},t)dt$ with a variable time step dt chosen inversely proportional to the maximum value of the resistivity $\rho=|E|/|J|$ on the grid at time t.

Next I generalize this method to general dependence $\mathbf{H}=\mathbf{H}(\mathbf{B},\mathbf{r})$. It turns out that this is achieved by replacing in $\mathbf{E}(\mathbf{J},\mathbf{B},\mathbf{r})$ in Eq. (3) the $\mathbf{J}=\mu_0^{-1}\nabla\times\mathbf{B}$ by the current density $\mathbf{J_H}=\nabla\times\mathbf{H}$ which drives the vortices and thereby generates the electric field $\mathbf{E}$. That $\mathbf{J_H}=\nabla\times\mathbf{H}(\mathbf{B},\mathbf{r})$ enters the Lorentz force is rigorously proven by Labusch.[7] Within the London theory this important relation may also be concluded from the facts that the force on a vortex is determined by the *local* current density at the vortex center, while the energy density F of the vortex lattice is determined by the magnetic field at the vortex centers. Thus, $\mathbf{J_H}=\nabla\times(\partial F/\partial\mathbf{B})$ is the average current density at the vortex centers, which in general is different from the current density $\mathbf{J}=\mu_0^{-1}\nabla\times\mathbf{B}$ averaged over several vortex spacings. Therefore, one has to replace in Eq. (3)

$$\mathbf{E}(\mathbf{J},\mathbf{B},\mathbf{r}')\rightarrow\mathbf{E}[\mathbf{J_H}(\mathbf{r}',t),\mathbf{B}(\mathbf{r}',t),\mathbf{r}'], \tag{4}$$

where $\mathbf{J_H}=\nabla\times\mathbf{H}$ depends on the material law $\mathbf{H}=\mathbf{H}(\mathbf{B},\mathbf{r})=\partial F/\partial\mathbf{B}$. The *boundary condition* on $\mathbf{H}(\mathbf{r})$ is simply that one has $\mathbf{H}=\mathbf{B}/\mu_0$ at the surface (and in the vacuum outside the superconductor, which does not enter our calculation). The boundary conditions on $\mathbf{H}$ and $\mathbf{B}$ are now contained in the space-dependent material law $\mathbf{H}=\mathbf{H}(\mathbf{B},\mathbf{r})$ and in the relation $\mathbf{B}=\nabla\times\mathbf{A}$, which guarantees that $\nabla\cdot\mathbf{B}=0$ in all space. The specimen shape thus enters in two places: via the integral kernel $K(\mathbf{r},\mathbf{r}')$ and via the material law $\mathbf{H}=\mathbf{H}(\mathbf{B},\mathbf{r})$. The kernel $Q(\mathbf{r},\mathbf{r}')$ and its derivative $\mathbf{L}(\mathbf{r},\mathbf{r}')=-\nabla_\mathbf{r}Q(\mathbf{r},\mathbf{r}')$ do not depend on the specimen shape. The kernel $\mathbf{L}(\mathbf{r},\mathbf{r}')$ enters the Biot-Savart law

$$\mathbf{B}(\mathbf{r})=\int_V d^3r'\mathbf{L}(\mathbf{r},\mathbf{r}')\times\mathbf{J}(\mathbf{r}')+\mathbf{B_a}(\mathbf{r}), \tag{5}$$

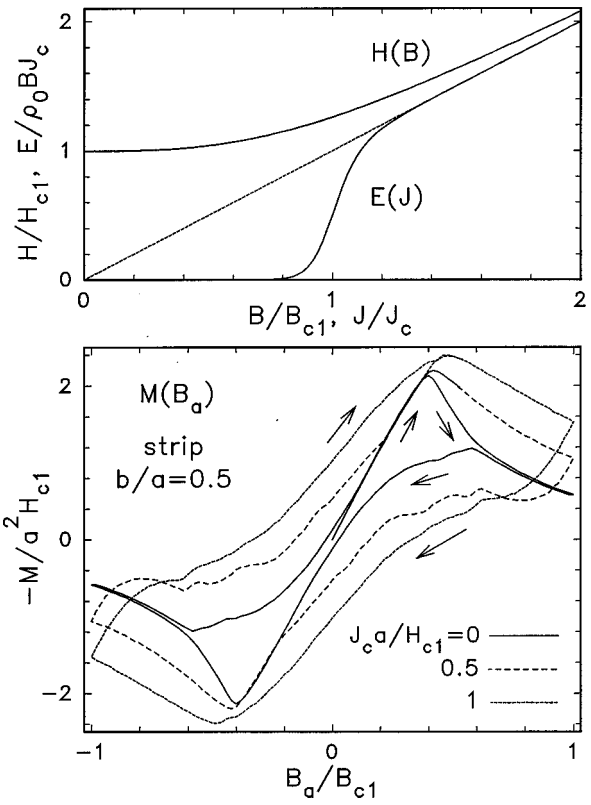

FIG. 1. Top: The models $H(B)$, Eq. (6), and $E(J,B)$, Eq. (7), with $\sigma=20$. Bottom: Magnetization loops $M=\mathbf{m}\hat{\mathbf{y}}$ (per unit length in units a^2H_{c1}) of a strip with $b/a=0.5$ and finite H_{c1} versus the cycled applied field B_a for various volume pinning strengths $J_c=0$, 0.5, and 1 (in units H_{c1}/a).

which should be used to compute the $\mathbf{B}(\mathbf{r})$ entering $\mathbf{H}(\mathbf{B},\mathbf{r})$. The accuracy of the method then depends mainly on the algorithm used to compute the derivative $\mathbf{J_H}=\nabla\times\mathbf{H}$. A useful trick is to compute $\mathbf{J_H}$ as $\mathbf{J_H}=\mathbf{J}+\nabla\times(\mathbf{H}-\mathbf{B}/\mu_0)$ where $\mathbf{H}-\mathbf{B}/\mu_0$ is typically small and vanishes at the surface, albeit with a jump. The magnetic moment of the superconductor is

$$\mathbf{m}=\frac{1}{2}\int_V\mathbf{r}\times\mathbf{J}(\mathbf{r})d^3r. \tag{6}$$

Equations (1)–(6) are still general. For the following computations I shall use simple models for an isotropic homogeneous type-II superconductor without Hall effect, for which $\mathbf{H}(\mathbf{B})=H(B)\mathbf{B}/B$ $(B=|\mathbf{B}|)$ and $\mathbf{E}(\mathbf{J},\mathbf{B})=\rho(J,B)\mathbf{J}$. I chose the models (Fig. 1)

$$H(B)=[H_{c1}^\alpha+(B/\mu_0)^\alpha]^{1/\alpha} \tag{7}$$

with $\alpha=3$ (better magnetization curves may be taken from the Ginzburg-Landau solution of Ref. 12) and

$$\rho(J,B)=\rho_0B\frac{(J/J_c)^\sigma}{1+(J/J_c)^\sigma}, \tag{8}$$

which has the correct limits $\rho\propto J^\sigma$ $(J\ll J_c$, flux creep) and $\rho=\rho_0B$ $(J\gg J_c$, flux flow, $\rho_0=$ const). In general the critical current density $J_c=J_c(B)$ and the creep exponent $\sigma(B)\geqslant 0$ may depend on B.

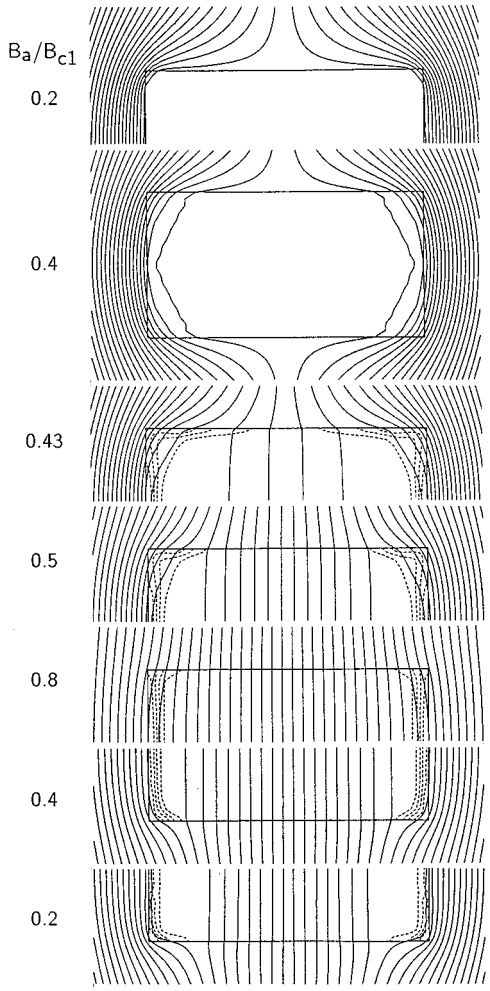

FIG. 2. Magnetic field lines of a pin-free ($J_c=0, B_{c1}>0$) superconductor long strip with side ratio $b/a=0.5$ in increasing and then decreasing perpendicular field $B_a(t)/B_{c1}=0\rightarrow 1\rightarrow -1$ (from top to bottom, see text). First flux jumps to the center at $|B_a|/B_{c1}=0.4$. The dashed lines are the contours of the current density $J(x,y)$.

I now apply this method to long superconductor strips of rectangular cross section ($|x|\leqslant a, |y|\leqslant b$) in a perpendicular field $\mathbf{B_a}=B_a(t)\hat{\mathbf{y}}$ with no applied current. In this geometry $\mathbf{J}=J(x,y)\hat{\mathbf{z}}$, $\mathbf{E}=E(x,y)\hat{\mathbf{z}}$, and $\mathbf{A}=A(x,y)\hat{\mathbf{z}}$ have only one component and $\mathbf{B}=B_x(x,y)\hat{\mathbf{x}}+B_y(x,y)\hat{\mathbf{y}}$ and $\mathbf{H}(\mathbf{B})=\mathbf{B}H(B)/B$ have two. The required 2D integral kernel $Q(x,y;x',y')=(\mu_0/2\pi)\ln|\mathbf{r}-\mathbf{r}'|$ is obtained by integrating the 3D kernel $Q(\mathbf{r},\mathbf{r}')=\mu_0/(4\pi|\mathbf{r}-\mathbf{r}'|)$ along z'. Accounting for the symmetry $J(x,y)=-J(-x,y)=J(x,-y)$ one arrives at the kernel $Q_{\rm sym}(x,y;x',y')$, Eq. (8) of Ref. 10. We may thus use the same numerical method as in Refs. 10 and 11, where also the extension to short cylinders in an axial field is described, and insert some new steps which compute from J the required $J_H=[\nabla\times\mathbf{H}(\mathbf{B})]\cdot\hat{\mathbf{z}}$.

Here I present some selected results obtained with constant J_c and $\sigma=20$. The four input parameters are now b/a (aspect ratio), H_{c1} (lower critical field), J_c (volume pinning), and σ (creep exponent). In units $a=\mu_0=1$ with ramp rate $|\dot{B}_a|=1$, I chose $\rho_0=40$ in Eq. (8) if $J_c\neq 0$ but $\rho_0=200$ (large flux flow rate) if $J_c=0$ to ensure complete relaxation

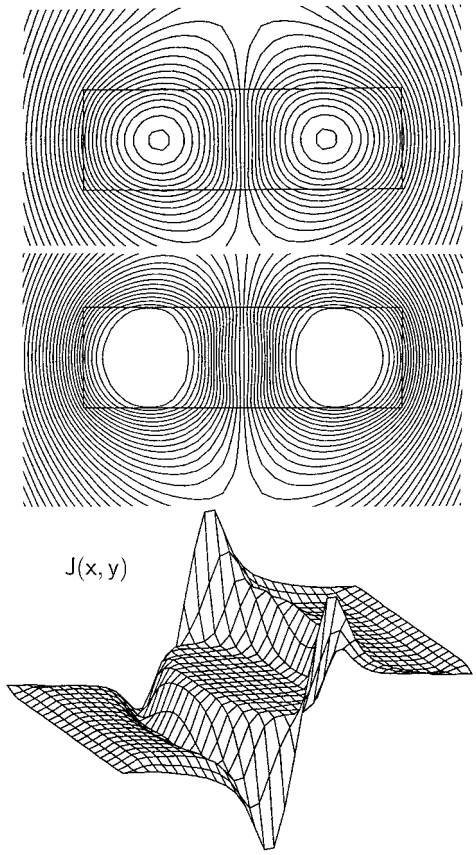

FIG. 3. Magnetic field lines of a superconductor strip with $b/a=0.3$ and strong pinning after increasing and then decreasing the field $B_a/(\mu_0 J_c a)=0\rightarrow 0.44\rightarrow -0.08$ for $H_{c1}=0$ (top) and $H_{c1}=aJ_c/5$ (middle). Bottom: Current density $J(x,y)$ in a strip with $b/a=0.5, J_c>0$, and $H_{c1}=aJ_c/4$ in increasing field $B_a=0.35\mu_0 J_c a=1.4B_{c1}$.

to the pin-free static solution. The program allows us to monitor the flux motion in real time, but high accuracy is still difficult to achieve.

Figure 1 shows three magnetization loops $M(B_a)$ of strips with $b/a=0.5$ and finite $B_{c1}=\mu_0 H_{c1}$ for $J_c=0$, 0.5, and 1 in units of H_{c1}/a. Note the asymmetric hysteresis in the absence of volume pinning ($J_c=0$), which reflects the *geometric barrier*. Finite J_c broadens this hysteresis nearly symmetrically about the pin-free curve at $|B_a|>B_{c1}$. For $J_c=0$ the maximum magnetic moment $|M|$ occurs at almost the same field $B_{\rm en}$ where the first flux lines enter and jump to the center of the strip. For $b/a=0.2$ (0.3, 0.5, 0.7, 1, 1.4, 2, 3, 4, 5, 7, 10) this entry field is $B_{\rm en}=B_{c1}\times 0.247$ (0.304, 0.396, 0.465, 0.541, 0.611, 0.682, 0.745, 0.796, 0.834, 0.882, 0.910). In the thin-strip limit $b\ll a$, I find $B_{\rm en}/B_{c1}=0.56\sqrt{b/a}$. A good fit for all aspect ratios $0<b/a<\infty$ is

$$B_{\rm en}\approx B_{c1}\tanh\sqrt{0.36b/a}. \tag{9}$$

This computed entry field for rectangular strips has the correct limit $B_{\rm en}\propto\sqrt{b/a}$ for $b\ll a$, but it is smaller than previous thin-strip estimates $B_{\rm en}/B_{c1}=(0.95\cdots 1)\sqrt{b/a}$.[3,6] It is still much larger than the entry field of strips with elliptical cross section, $B_{\rm en}/B_{c1}=b/(a+b)\rightarrow b/a$ for $b\ll a$.[13] For disks with radius a the constant 0.36 in Eq. (9) is replaced by 0.67.

The magnetic field in the pure Meissner case $J_c=0$ is shown in Fig. 2 for a thick strip with $b/a=0.5$ in cycled field

$B_a(t)/B_{c1}=0\rightarrow 1\rightarrow -1\rightarrow 1$, etc. The strip cross section is shown as a rectangle $2a\times 2b$, or its half $2a\times b$ to save space. Inside the superconductor the magnetic field lines (contour lines of A) may be interpreted as Abrikosov flux lines, which enter and leave the strip and rapidly jump across flux free zones.

One can see that the magnetic flux penetrates from the rectangular corners in form of nearly straight flux lines inclined at $\approx 45°$. When the flux lines join at the equator at $B_{\rm en}=0.4B_{c1}$, flux jumps to the center and piles up in form of *almost straight and equidistant flux lines* which means near zero current density J in the volume (J_H exactly vanishes). During the entire cycle the current flows mainly near the short edges $x=\pm a$. With decreasing $B_a(t)$ the flux exits delayed but has completely left at $B_a=0$ (if $\rho_0/|\dot{B}_a|$ is large), i.e, there is no remanent static flux. With further decrease of B_a the picture exactly repeats but with J and B of opposite sign. Weak volume pinning (not shown) delays this penetration and exit of flux and splits the central pile of flux into two piles with steep slope on the inner side as predicted by Zeldov *et al.*[3] Our computation thus confirms the edge-barrier scenario suggested in Refs. 3–8.

Evidence for the ''current string''[9] can be seen in Fig. 3. The depicted magnetic field lines in a strip with $b/a=0.3$ and strong volume pinning, in decreasing field $B_a/(\mu_0 J_c a)=0\rightarrow 0.44\rightarrow -0.08$ indicate a much stronger local current density if $H_{c1}=J_c a/5$ is finite (middle of Fig. 3) than if $H_{c1}=0$ (top). The bottom of Fig. 3 shows the current density $J(x,y)$ of a strip with $b/a=0.5$ and $H_{c1}=0.25J_c a$ in increasing field $B_a/B_{c1}=0\rightarrow 1.4$. Note the ridge of enhanced $J(x,y)$ at the penetrating flux front where the three plateaus $J=-J_c$, 0, $+J_c$ (left to right) border each other. Also seen is the weak Meissner current at the surfaces. As an interesting feature, four sharp peaks of $J(x,y)$ are seen close to the poles of the strip (near the lines $x=0, y=\pm b$). All these enhancements of $J(x,y)$ are absent in the previous approximation $\mathbf{B}=\mu_0\mathbf{H}$, where $J(x,y)$ exhibits only the plateaus 0 and $\pm J_c$.

[1] L. Burlachkov, Phys. Rev. B **47**, 8056 (1993).

[2] J. Provost, E. Paumier, and A. Fortini, J. Phys. F **4**, 439 (1974); A. Fortini, A. Hairie, and E. Paumier, Phys. Rev. B **21**, 5065 (1980); A. V. Kuznetsov, D. V. Eremenko, and V. N. Trofimov, *ibid.* **57**, 5412 (1998).

[3] E. Zeldov, A. I. Larkin, V. B. Geshkenbein, M. Konczykowski, D. Majer, B. Khaykovich, V. M. Vinokur, and H. Shtrikman, Phys. Rev. Lett. **73**, 1428 (1994); E. Zeldov *et al.*, Physica C **235-240**, 2761 (1994).

[4] Th. Schuster, M. V. Indenbom, H. Kuhn, E. H. Brandt, and M. Konczykowski, Phys. Rev. Lett. **73**, 1424 (1994).

[5] I. L. Maksimov and A. A. Elistratov, Pis'ma Zh. Éksp. Teor. Fiz. **61**, 204 (1995) [JETP Lett. **61**, 208 (1995)].

[6] M. Benkraouda and J. R. Clem, Phys. Rev. B **53**, 5716 (1996); N. Morozov *et al.*, Physica C **291**, 113 (1997); A. V. Kuznetsov *et al.*, Phys. Rev. B **56**, 9064 (1997).

[7] R. Labusch and T. B. Doyle, Physica C **290**, 143 (1997); T. B. Doyle, R. Labusch, and R. A. Doyle, *ibid.* **290**, 148 (1997).

[8] M. V. Indenbom *et al.*, Physica C **222**, 203 (1994); M. V. Indenbom and E. H. Brandt, Phys. Rev. Lett. **73**, 1731 (1994); E. H. Brandt, Rep. Prog. Phys. **58**, 1465 (1995).

[9] M. V. Indenbom, Th. Schuster, H. Kuhn, H. Kronmüller, T. W. Li, and A. A. Menovsky, Phys. Rev. B **51**, 15 484 (1995).

[10] E. H. Brandt, Phys. Rev. B **54**, 4246 (1996).

[11] E. H. Brandt, Phys. Rev. B **58**, 6506 (1998); **58**, 6523 (1998).

[12] E. H. Brandt, Phys. Rev. Lett. **78**, 2208 (1997).

[13] R. P. Huebener, R. T. Kampwirth, and J. R. Clem, J. Low Temp. Phys. **6**, 275 (1972).